LC-balun impedance matching for a mixer first RF front-end

Martijn B. Bes

***Abstract*— An LC-balun for application with a passive mixer first RF front-end is proposed. It uses the common grounded differential load in the RF front-end to achieve a 178.5±2.9 degrees phase-difference and has wideband characteristics due to the use of a separate low-pass and high-pass impedance matching network. Furthermore, an S_{11} of -7.5dB at a center frequency of 1GHz is achieved, with a peak of -24dB at 990MHz.**

Keywords—LC-balun, impedance matching, RF front-end

I. Introduction

Passive mixer-first receiver architecture for RF front-ends have become increasingly common over the last decade due to high linearity and tunability[1]. These front-ends often use a mixer called N-path filter at their input, which in most cases has a differential input to get rid of even harmonics[1]. To create a differential output from a single input a balun is needed.

The balun is a device or circuit that is designed to either convert a balanced to an unbalanced signal or the other way around, in this paper only unbalanced to balanced transformation is of interest. For a balun a transformer or microwave circuit can be used[2] [3]. The balun also accounts for impedance matching, which is necessary for maximum power transfer, as explained in II.A. These types of balun have a very wide bandwidth and microstrips especially often require a highly specific design. Furthermore baluns based on half or quarter wavelength section can become quite big at around 1 GHz, as this frequency results in a quarter wavelength of almost 5.5 cm, resulting in a Marchand balun at 1 GHz having a minimum length of 11 cm[2]. This becomes less of a problem at high enough frequencies, as the wavelength scales inversely with the frequency.

Another way to achieve impedance matching is by using LC-based networks, as they can be made to have a high Q (Q > 10), and thus a small bandwidth. However, these networks do not achieve the balun requirement as they are single-ended networks. Another option is the LC-balun network, an LC-based balun first introduced in the 1930's that also achieves impedance matching[4]. In literature this circuit could not be found to be used as an unbal for reasons discussed in this paper. The main goals are to find out whether this LC-balun, using lumped elements, can achieve a higher Q than a transformer/microstrip balun and whether this LC-balun can be applied to the aforementioned RF front-end.

In this paper the capability of an LC-balun network to convert a signal from unbalanced to balanced will be assessed. First by time invariant AC and S-parameter simulations and finally by periodic S-parameter simulation when connected to an ideal model of an RF front-end. In both the AC and S-parameter simulations the frequency range of interest is $f_0 \pm 16MHz$ (IF bandwidth of RF front-end), with f_0 being the center frequency at one gigahertz. This is the operating frequency at which the previously designed RF front-end works[5]. The other part that will be looked at is its wideband behavior to find the bandwidth and thus the Q-factor of the balun.

II. Impedance Matching Theory

A. Maximum power transfer theorem

The maximum power transfer theorem states that to achieve a maximum power transfer from a source with internal impedance Z_{Source} to a load with input impedance Z_{Load} these impedances should be complex conjugates of each other[6]. For real impedances this implies (1).

$$R_{Source} = R_{Load} \tag{1}$$

To match complex impedances a capacitor or inductor in series or parallel with the to be matched impedance can be used. Since the capacitor's and inductor's impedance is frequency dependent, according to (2), the circuit is only perfectly matched at one frequency, the center frequency f_0.

$$Z_C = -\frac{j}{2\pi fC}, Z_L = j2\pi fL \tag{2}$$

B. RF front-end model

The RF front-end mentioned in the introduction can be modelled as a passive RC network, consisting of both a series RC circuit and a parallel RC circuit, shown in Fig. 1. In the top model the RC series circuit is comprised of the source resistance, R_S, and the parasitic capacitance, C_P, which is the equivalent parasitic capacitance of capacitances $C_1 - C_4$, with value C. Since each capacitor has two parasitic capacitors, $C_P = 8C$. When going from time variant to time invariant the capacitors with switches can be modelled as a parallel shunt resistance and a capacitance[7]. The capacitance C_x is the LTI equivalent of C_{1-4}, and the shunt resistance R_{shunt} is the equivalent resistance looking from V_x, created by the switch resistance, R_{sw}, and a frequency dependent harmonic loss due to R_s and C_P. For ease of analysis and a demonstration of the behavior of the LC-balun only a real load impedance is used, to simulate a step-up transformation, similar to a step-up transformer balun.

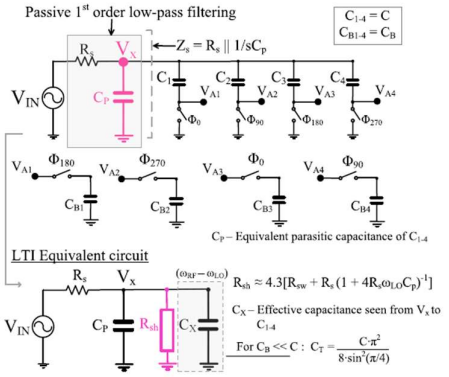

Figure 1: Model of RF front-end, top: time variant model, bottom: time invariant equivalent model[7]

C. LC-balun analysis

The LC-balun consists of a high-pass filter which creates a phase shift of +90 degrees and a low-pass filter which creates a phase shift of -90 degrees, shown in Fig. 2.

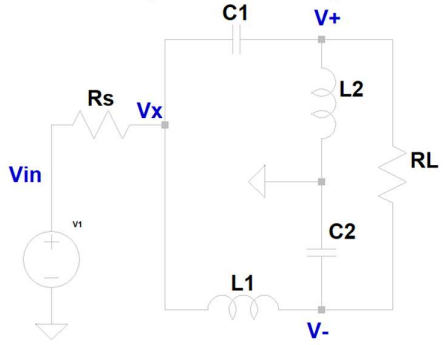

Figure 2: LC-balun circuit with differential load

When using both filters a 180-phase difference can be created between the outputs of the filters, thus achieving a balanced output signal. This design is normally only used for circuit with extremely high load impedances such as driving MOS-transistor gates[8]. In (3) and (4) the transfer functions $\frac{V_+}{V_{in}}$ and $\frac{V_-}{V_{in}}$ are shown, from this (5) and (6) can be derived. These equations show that only for $R_L \to \infty$, a 180 degree phase-difference can be achieved between φ_{V_+} and φ_{V_-} [9]. X is the reactance of L and C and is determined by (7).

$$\frac{V_+}{V_{in}} = \frac{\frac{1}{2}R_L + jX}{jX} \tag{3}$$

$$\frac{V_-}{V_{in}} = -\frac{\frac{1}{2}R_L - j}{jX} \tag{4}$$

$$\varphi_{V_+} = \arctan\left(\frac{X}{R_L}\right) - \arctan\left(\frac{X}{0}\right) = \arctan\left(\frac{X}{R_L}\right) - \frac{\pi}{2} \tag{5}$$

$$\varphi_{V_-} = \arctan\left(\frac{X}{-R_L}\right) - \arctan\left(\frac{-X}{0}\right) = -\arctan\left(\frac{X}{R_L}\right) + \frac{\pi}{2} \tag{6}$$

$$X = 2\pi f_o L = \frac{1}{2\pi f_o C} \tag{7}$$

Since a finite load is used in the RF front-end this circuit design on its own will not work. However, from simulations it was noticed that once a common mode voltage is set at the differential load, the 180-degree phase-difference can be achieved. Since the common mode voltage is set to zero for the RF front-end the circuit used for simulation and analysis contains a common ground, as shown in Fig. 3.

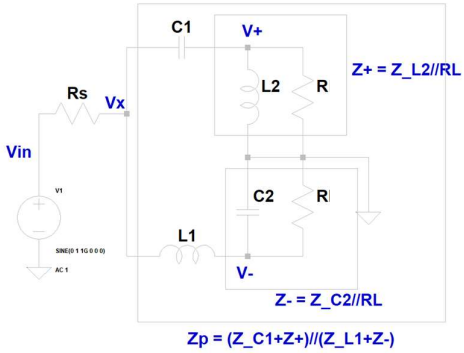

Figure 3: LC-balun with a common mode voltage defined by the ground, V_{cm}= 0V.

In Fig. 3 the differential load is split into two resistors of half the value of the load impedance. To analyze the circuit, it is broken up into equivalent impedances. Then using circuit analysis, the following expressions (8), (9) and (10) are found. The equivalent impedance Z_P is shown in (11).

$$\frac{V_x}{V_{in}} = \frac{Z_P}{R_S + Z_P} \tag{8}$$

$$\frac{V_+}{Vx} = \frac{Z_+}{Z_{C1} + Z_+} \tag{9}$$

$$\frac{V_-}{Vx} = \frac{Z_-}{Z_{L1} + Z_-} \tag{10}$$

$$Z_P = \frac{Z_L Z_C (R+Z_L)(R+Z_C) + RZ_L^2(R+Z_C) + RZ_C^2(R+Z_L) + R^2 Z_L Z_C}{Z_L(R+Z_L)(R+Z_C) + Z_C(R+Z_L)(R+Z_C) + RZ_L(R+Z_C) + RZ_C(R+Z_L)} \tag{11}$$

For maximum power transfer, the source resistance R_S must equal the impedance Z_P as this means that the power delivered to Z_P is equal to the power dissipated by the source resistance. This implies that only if Z_P is real, maximum power transfer can be achieved, unless the source resistance is a complex impedance rather than a real resistance. This results in (11) which is the requirement for maximum power transfer. The second equation that needs to hold is (12), this is because having a purely imaginary transfer from V_x to V_+ and V_x to V_- results in a 90 degree phase-shift, (13). When $\frac{V_+}{V_x}$ and $\frac{V_-}{V_x}$ are conjugates this results in a positive 90 degree phase-shift at V_+ and a negative 90 degree phase-shift at V-, which results in the wanted 180 degree phase-difference. For (12) to hold (15) must be true.

$$R_s = Z_P \tag{11}$$

$$Re\left\{\frac{V_+}{V_x}\right\} = Re\left\{\frac{V_-}{V_x}\right\} = 0,\ Im\left\{\frac{V_+}{V_x}\right\} = -Im\left\{\frac{V_-}{V_x}\right\} \tag{12}$$

$$\varphi_{V_+} = \arctan\left(\frac{Im\left\{\frac{V_+}{V_x}\right\}}{Re\left\{\frac{V_+}{V_x}\right\}}\right) = \arctan\left(\frac{Im\left\{\frac{V_+}{V_x}\right\}}{0}\right) = \frac{\pi}{2} \tag{13}$$

$$\varphi_{V_-} = \arctan\left(\frac{Im\left\{\frac{V_-}{V_x}\right\}}{Re\left\{\frac{V_-}{V_x}\right\}}\right) = \arctan\left(\frac{Im\left\{\frac{V_-}{V_x}\right\}}{0}\right) = -\frac{\pi}{2} \tag{14}$$

$$Z_L = -Z_C \tag{15}$$

Solving (11) for L and C with the constraints (12) and (15) results in equations (15) and (16) for L and C, dependent on frequency, load impedance, and source impedance.

$$L = \frac{\sqrt{R_S R_L}}{\omega_1} \tag{16}$$

$$C = \frac{1}{\omega\sqrt{R_S R_L}} \tag{17}$$

This shows that in theory the LC-balun with a common mode of zero volts, can be used at any frequency for any real load and source impedance. However, when the to be matched impedances are complex a complex value for L and C is required, this can be solved by cancelling the imaginary part of the load resistance with an imaginary impedance of the opposite sign. If this is not done the 180-degree phase-difference cannot be achieved for complex loads.

D. Impact of non-idealities

There are two non-idealities to be considered:

1. Tolerance
2. Q-factor

The tolerance influences both the center frequency and the matching, it influences (11), (15) and (18). The center frequency of the circuit is defined by (18).

$$f_0 = \frac{1}{2\pi\sqrt{LC}} \tag{18}$$

This implies that the frequency varies with respect to the inverse quadratic relationship with both L and C. Since the center frequency shifts away from the ideal center frequency when a tolerance is applied, the ideal matching now occurs at the new center frequency, resulting in a mismatch at the wanted center frequency.

The Q-factor of the lumped elements influence the matching and phase-difference. The Q-factor represents a parasitic series resistance for an inductor and parallel resistance for a capacitor according to (19) and (20) respectively.

$$Q_{ind} = \frac{2\pi f_0 L}{R_{par,ind}} => R_{par,ind} = \frac{2\pi f_0 L}{Q_{ind}} \tag{19}$$

$$Q_{cap} = 2\pi f_0 C R_{par,cap} => R_{par,cap} = \frac{Q_{cap}}{2\pi f_0 C} \tag{20}$$

This makes Z_L and Z_C complex rather than purely imaginary with values, $Z_L = j2\pi fL + R_{par,ind}$ and $Z_C = \frac{R_{par,cap}}{j2\pi f R_{par,cap} C+1}$, which results in a mismatch of impedances (15) and a smaller than 180-degree phase-difference. Since a higher Q-factor implies a lower series and a higher parallel resistance, this means that for a higher Q the impedance mismatch and phase imbalance will be lower.

III. Circuit design

As mentioned in the theory, the LC-balun network will be used as the matching network. Since all equations have been previously derived the design, the necessary component values can now be acquired. Setting the center frequency at 1GHz and setting the impedances to $R_s = 50\Omega$, $R_L = 200\Omega$ this results in $L = 15.92nH$ and $C = 1.592pF$. Since such a precise value is often not available for a lumped element the design will also be simulated for $L = 16nH \pm 0.8nH$ and $C = 1.6pF \pm 0.02pF$, the inductor has a 5% tolerance whilst the capacitor has a tolerance of ±0.02pF, these are tolerances which can be found in commercially available components[10][11]. These new values for L and C will result in a lower center frequency (at nominal value). $f_{0,nom} = \frac{1}{2\pi\sqrt{16nH*1.6p}} = 994.7MHz$.

A Q of 50 is chosen for the inductor as this is a common value for RF inductors[10], this results in a parasitic series resistance of $R_{par,ind} = \frac{2\pi*1GHz*16nH}{50} = 2.01\Omega$.

For the capacitor, a Q of 300 is chosen[11]. The Q is defined to be at a frequency of 1 GHz. This results in a parasitic parallel resistance of $R_{par,cap} = \frac{300}{2\pi*1GHz*1.6pF} = 29.84k\Omega$.

The expected voltage at V_+ and V_- can now be calculated for both the ideal and non-ideal elements, from (8), (9) and (10). For the ideal case:

$Z_P = 50\Omega$ resulting in $\frac{V_x}{V_{in}} = 0.5$, $\frac{V_+}{V_x} = 1j$, and $\frac{V_-}{V_{in}} = -1j$, resulting in $\left|\frac{V_+}{V_{in}}\right| = \left|\frac{V_-}{V_{in}}\right| = 0.5$.

And $\varphi_{V_+} = \arctan\left(\frac{1}{0}\right) = \frac{\pi}{2}$ and $\varphi_{V_-} = \arctan\left(\frac{-1}{0}\right) = -\frac{\pi}{2}$.

Resulting in a phase-difference of π or 180 degrees.

For the non-ideal case:

$Z_P = 50.6\Omega - 0.8j\Omega$ resulting in $\frac{V_x}{V_{in}} = 0.497 + 0.004j$, $\frac{V_+}{V_x} = 0.004 + 0.977j$, and $\frac{V_-}{V_{in}} = 0.019 - 0.977j$, resulting in $\left|\frac{V_+}{V_{in}}\right| = \left|\frac{V_-}{V_{in}}\right| = 0.486$.

With $\varphi_{V_+} = \arctan\left(\frac{0.977}{0.004}\right) = 1.5671 \approx 89.8\ deg$ and $\varphi_{V_-} = \arctan\left(\frac{-0.977}{0.019}\right) = -1.551 \approx -88.9\ deg$, resulting in a phase-difference of 178.7 degrees. For these calculations, a matlab script was created, which can be found in the appendix.

Since the balun consists of a separate high-pass and low-pass filter rather than two band-pass filters, a small bandwidth cannot be achieved, as no real band-pass behavior occurs. The reason no band-pass filter was used is because there are no LC-based band-pass filters exist that can both achieve a 90-degree phase shift and account for impedance matching/conversion. The one LC-based band-pass filter that achieves impedance matching consists of two consecutive LC filters, as shown in Fig. 3. The transfer from before C_s to after C_s will be purely imaginary and the transfer from before L_L to after L_L will also be purely imaginary, but of opposite sign(as the opposite configurations give opposite behavior). This ensures the phase-shift from before C_s to after L_L will not be 90 degrees. As the first part of the filter will already create the 90-degree phase-shift whilst the second part will change this to a different value.

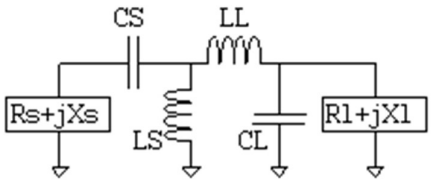

Figure 4: LC-based bandpass impedance matching network[12]

IV. Simulation results and Discussion

To test the performance of the LC-balun, simulations were done in SpectreRF. For AC analysis and S-parameter analysis two different circuits will be used visible in Fig. 5 and Fig. 10. For analysis with the RF front-end the same circuit is used as in Fig. 5, however the load resistors are now replaced with the time-variant RF front-end, the RF front-end model can be found in the appendix. First an AC analysis is done to determine the phase-difference, differential gain, and the bandwidth. After that, a time-invariant S-parameter simulation was done to determine S_{11}, followed by a time-

variant periodic S-parameter simulation to determine S_{11} when connected to an idealized model of an RF front-end. S-parameter S_{11} represents the fraction of power reflected with respect to the power coming from the source (port 1).

A. Simulation with ideal components

1) AC analysis

First an AC analysis of the circuit was done to see if the voltage levels were as expected, and to determine the phase and differential gain, $\frac{V_+ - V_-}{V_{in}}$.

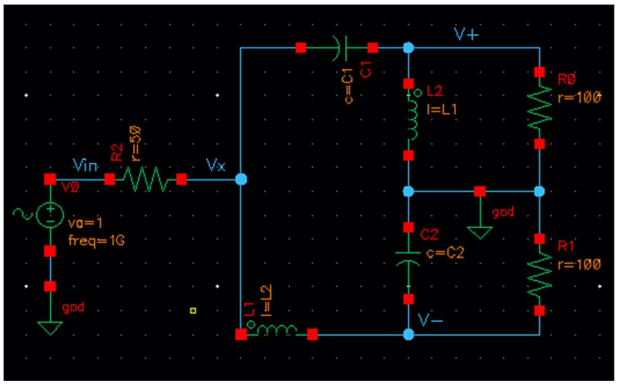

Figure 5: Schematic of circuit used for AC analysis

In Fig. 6 and Fig. 7 it can be seen that the magnitude of the transfer functions $\frac{V_+}{V_{in}}$ and $\frac{V_-}{V_{in}}$ are both at -6dB at 1 GHz, meaning that the amplitude of the voltage is half that of V_{in} which is as expected.

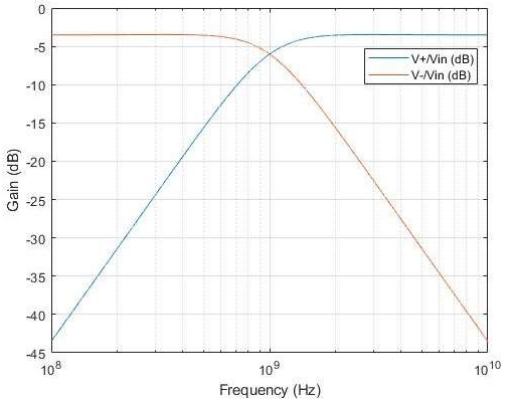

Figure 6: Magnitude of V+/Vin and V-/Vin versus frequency

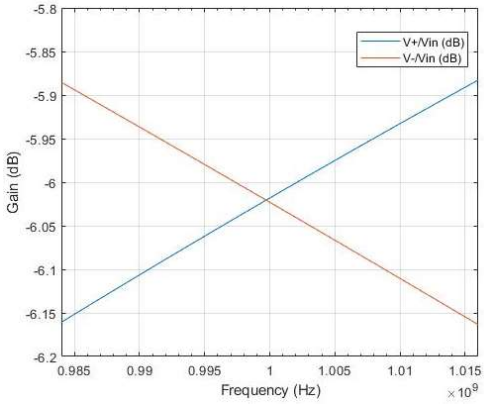

Figure 7: Magnitude of V+/Vin and V-/Vin across the IF bandwidth

In Fig. 8 and Fig. 9 the differential gain and phase are shown. The differential gain across the frequency spectrum from 100MHz to 10GHz -3.5dB to 0dB, as expected the differential gain is 0dB at 1GHz, meaning both V_+ and V_- have an equal magnitude, the -3dB bandwidth is 3.8GHz, from 250MHz to 4GHz, which makes the balun a wideband balun. The phase imbalance is 179.99±0.1 degrees across the spectrum of 100MHz to 10GHz, dipping to 179.98 around 1GHz.

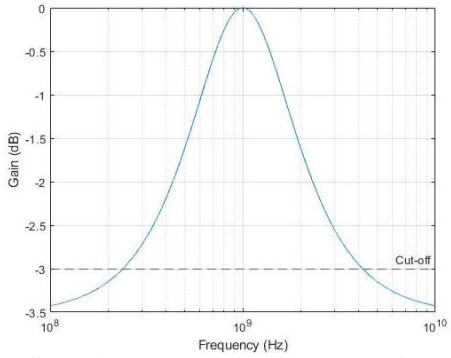

Figure 8: Differential gain across the frequency spectrum from 900MHz to 1100MHz

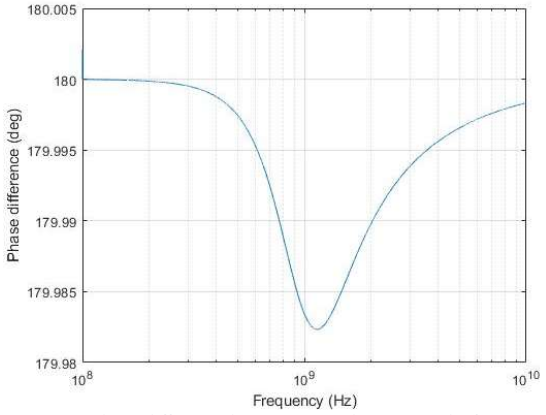

Figure 9: Phase-difference between V_+ and V_- across the frequency spectrum from 100MHz to 10 GHz

2) S-parameter simulations

In Fig. 11 and Fig. 12 the S-parameter S_{11} is shown. It represents the fraction of power reflected due to an impedance mismatch. At 1 GHz S_{11} is approximately -82dB, across the IF bandwidth S_{11} varies between -71dB and -82dB, this means that across the entire IF bandwidth only a small impedance mismatch occurs. From Fig. 11 for frequencies smaller than 900MHz and bigger than 1100MHz $S_{11} > -20dB$ meaning more than 1% of the power is reflected which implies an increasing impedance mismatch.

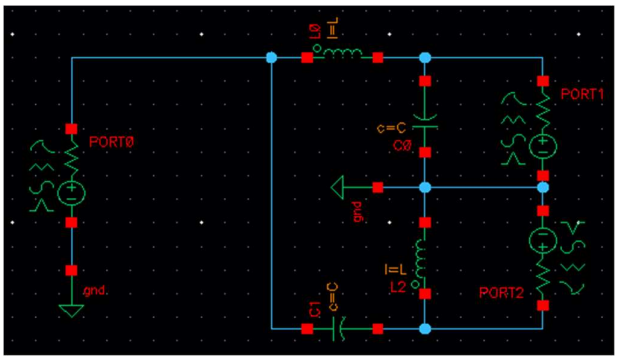

Figure 10: Schematic of the circuit used for S-parameter simulations

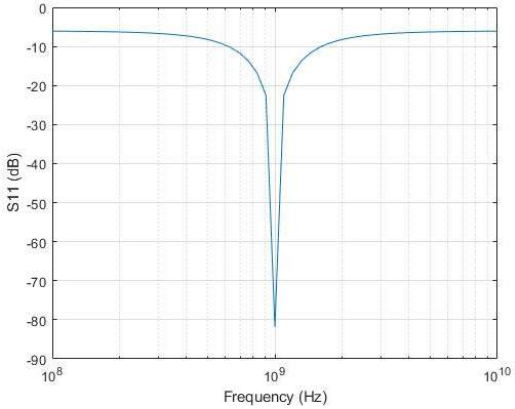

Figure 11: S_{11} across the frequency spectrum from 100MHz to 10GHz

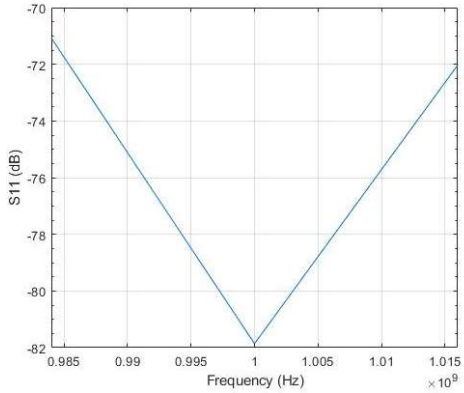

Figure 12: S_{11} across the IF bandwidth

B. Simulation with non-ideal components

For the simulations with non-ideal components only one components' value is changed at once, while keeping all other components at their nominal value. This is done to see how the tolerance influences the center frequency, differential gain, and phase-difference. Furthermore, the Q-factor negatively influence the differential gain. Simulations are done to see how much imbalance in the differential gain is created, by both the Q-factor and tolerance.

1) AC analysis simulations

In Fig. 13 the differential gain, $\frac{V_+ - V_-}{V_{in}}$, is shown across a frequency spectrum of 1±0.1 GHz. For these simulations only one component was changed whilst keeping the other three components at their nominal values. Here the gain imbalance is -155±5mdB at 1 GHz for a 5% variation in the inductor, whilst the gain imbalance at 1 GHz is -151mdB with negligible variance for a changing capacitor. The differential gain across the IF bandwidth is shown in Fig. 14 and Fig. 15.

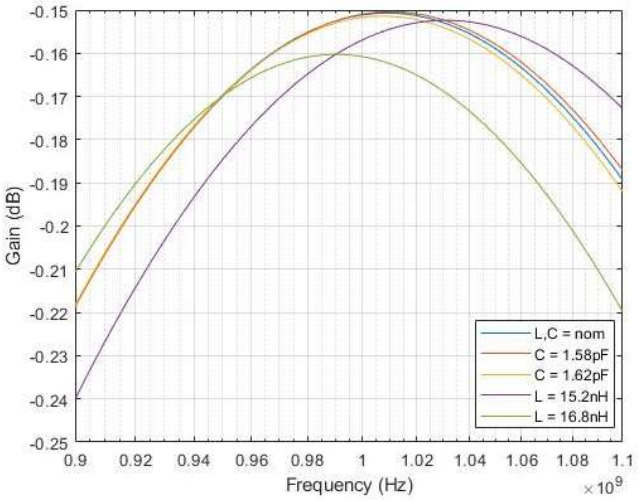

Figure 13: Differential gain across the frequency spectrum from 900 MHz to 1100MHz, for three inductor and capacitor values

Here it can be seen that the gain imbalance is -157.5±0.65mdB for a 5% variation in the inductor value and -152.5±20mdB for a changing capacitor across the IF bandwidth. From Fig. 16 the total phase-difference can be found. The phase-difference at 1 GHz is 178.6±2.8 degrees for a 5% variation in the inductor and 178.6±0.75 degrees for a changing capacitor. In Fig. 17 and Fig. 18 the phase-difference is shown across the IF bandwidth, it can be seen that across the IF bandwidth the phase-difference does not change, for a set component value.

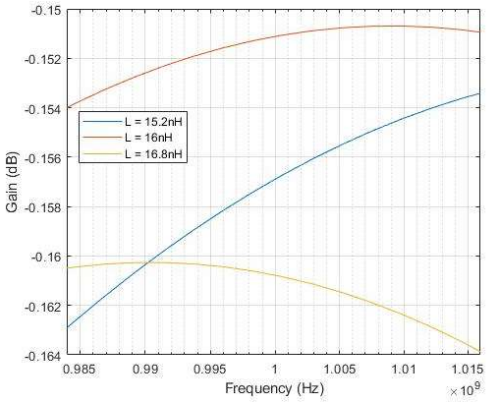

Figure 14: Differential gain across the IF bandwidth, at three inductor values

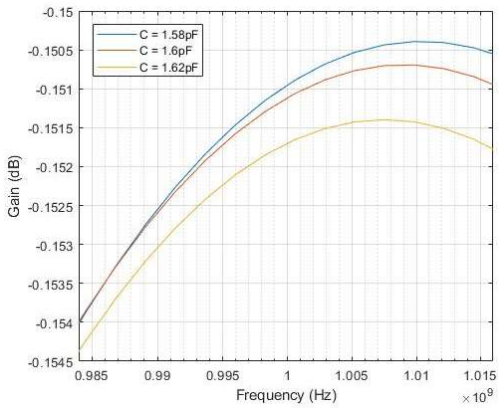

Figure 15: Differential gain across the IF bandwidth, at three capacitor values

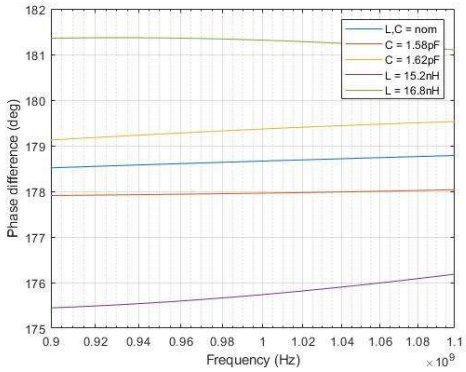

Figure 16: Phase difference across the frequency spectrum from 900 MHz to 1100 MHz, for three inductor and capacitor values

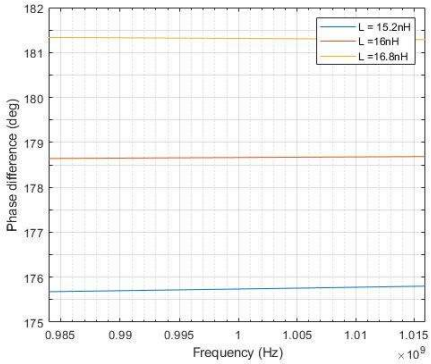

Figure 17: Phase difference across the IF bandwidth, for three inductor values

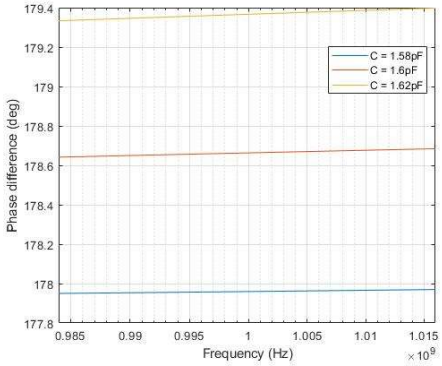

Figure 18: Phase difference across the IF bandwidth, for three capacitor values

Finally, the differential gain is plotted to show the -3dB bandwidth. The -3dB bandwidth is 3.7GHz, with the cut-off frequencies at 270MHz and 4GHz. This makes the LC-balun a wideband balun, as expected from the analysis.

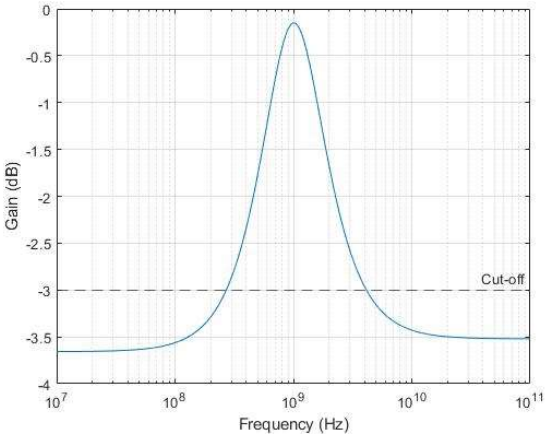

Figure 19: Differential gain versus frequency. For nominal L and C.

2) S-parameter simulations

In Fig. 20 and Fig. 21 the S-parameter S_{11} is shown at three different component values. The spread of S_{11} at 1 GHz is -36.5±5.5dB for a changing inductor and -41.5±2.5dB for a changing capacitor. The peaks shift in frequency from 1.005GHz to 1.02GHz for a changing capacitor, while the peaks frequency shift only a negligible amount for a changing inductor.

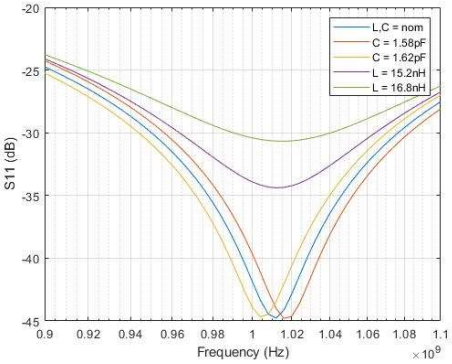

Figure 20: S_{11} across the frequency spectrum from 900MHz to 1100MHz, for three capacitor and inductor values

C. S-parameter simulation with RF front-end as load

In Fig. 22, S_{11} is shown across a frequency spectrum from 500MHz to 1500MHz as this is the original operating bandwidth of the RF front-end. These figures show a peak of -24dB at around 990MHz. In Fig. 23 the same curve is shown zoomed in on the IF bandwidth. Here it can be seen that the S_{11} is only below -20dB for frequencies around 990MHz, and this quickly increases. This means that the reflection loss only stays below 1% across a very small bandwidth, less than 10MHz. Outside of this small bandwidth the reflection loss rises to -2.5dB, which means that more than 70% of the power is lost due to reflection. Since the load is now both time-variant and complex it is expected that impedance matching with previously calculated values will not be optimal. Therefore, S_{11} was further simulated for different inductor and capacitor values. This was done by keeping either L or C at its original nominal value, while changing the other. The results are shown in Fig. 24 and Fig. 25. Here it can be seen that S_{11} reaches a low of -40dB and -42dB for a capacitor value of 1.3pF and an inductor value of 18nH, respectively. The same problem however still takes place, where the frequency range across which S_{11} stays below -20dB is less than the IF-bandwidth. This is primarily caused by the fact that the center frequency lies below 1GHz, resulting in a more asymmetric S_{11} across the IF bandwidth, like in Fig. 22.

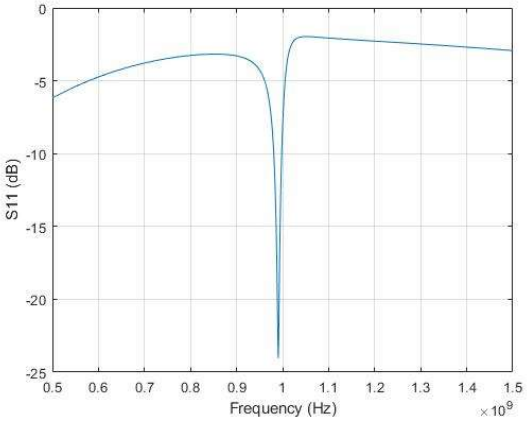

Figure 21: S_{11} across a frequency spectrum from 500MHz to 1500MHz, at nominal component value

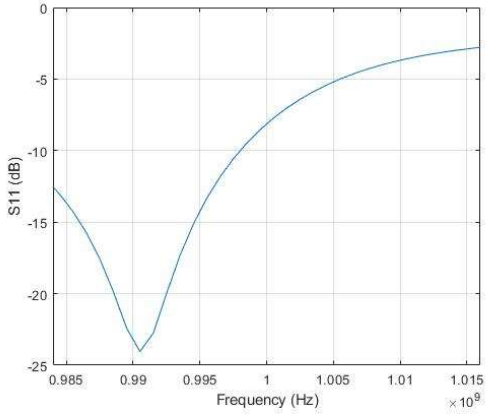

Figure 22: S_{11} across IF bandwidth, at nominal component values

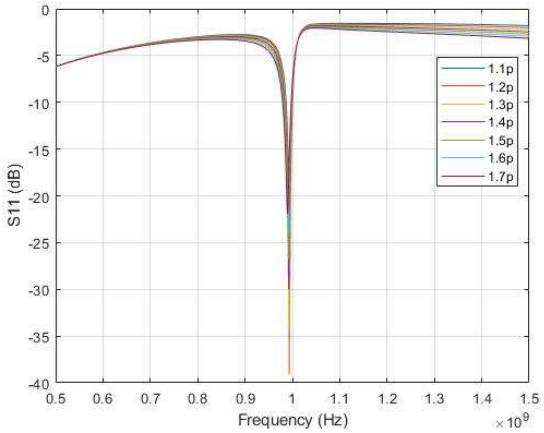

Figure 23: S_{11} versus frequency, simulated for different capacitor values, while keeping inductor at nominal value

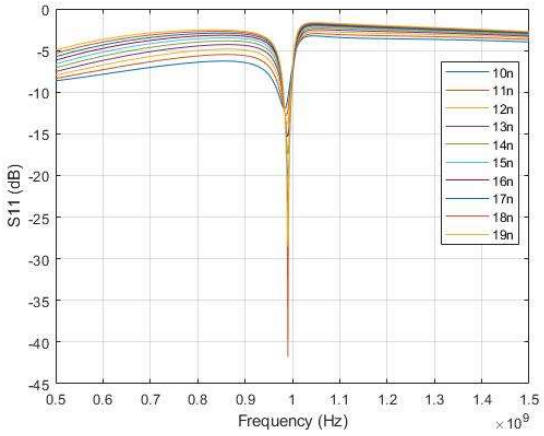

Figure 24: S_{11} versus frequency, simulated for different inductor values, while keeping capacitor at nominal value

D. Conclusions

1) AC analysis

The LC-balun has been successfully demonstrated to convert the unbalanced signal to a balanced signal when a common voltage of zero is defined at the differential load. Achieving a differential gain of -175mdB at 1GHz and a phase-difference of 178.5±2.9 degrees across the IF-bandwidth, for non-ideal components. A wideband balun with a -3dB bandwidth has been achieved.

2) Time-invariant S-parameter

The LC-balun achieves impedance matching and has been demonstrated to reduce reflection loss S_{11} to a low of -45 dB with spread of 10dB at 1GHz.

3) Time Variant (periodic) S-parameter

The LC-balun partially achieves impedance matching. S_{11} is below -20dB, meaning less than 1% power is lost around 990MHz. However, the impedance matching greatly diminishes across the rest of the IF bandwidth, to -2.5dB at 1016MHz, at which point most of the power is lost due to reflection. Compared to the time-invariant circuit the time-variant has a bigger impedance mismatch. This is because the time-invariant load resistance of 200Ω is only an approximation of the more complex time-variant model. As the time-variant model is more accurately represented by a complex valued time-invariant load. However, the value of

this time-invariant load is hard to determine as it depends on the value of the upconverted source resistance R_S. This means that your to be matched impedance depends on your matching network.

E. Recommendations

To improve the performance of the LC-balun for a time-variant circuit further research is required.

Since the load impedance of the RF front-end depends on the up-converted source impedance, R_S, this load impedance in turn depends on L and C. The equations in the analysis need to be adapted to the RF front-end model, taking the dependence of the to be matched load impedance on your LC-balun into account.

Furthermore, the LC-balun has not been tested in practice yet. This means that the simulations results done for this paper are only an approximation of the actual performance. For testing a lumped LC-balun network with SMD components with comparable characteristics, especially Q, needs to be built on a PCB. This was originally part of the research, however due to a lack of lab availability this could not be achieved and instead it was opted to use an idealized model of the RF front-end.

ACKNOWLEDGMENT

I would like thank supervisors E.A.M. Klumperink and V.K. Purushothaman for their help during the research and for providing the necessary RF front-end model.

REFERENCES

[1] E. A. M. Klumperink, H. J. Westerveld, and B. Nauta, "N-path filters and mixer-first receivers: A review," in *2017 IEEE Custom Integrated Circuits Conference (CICC)*, Austin, TX, Apr. 2017, pp. 1–8, doi: 10.1109/CICC.2017.7993643.

[2] D. Jorgesen and C. Marki, "Balun basics primer - A Tutorial on Baluns, Balun Transformers, Magic-Ts, and 180° Hybrids." Marki microwave, 2014, [Online]. Available: https://www.markimicrowave.com/Assets/appnotes/balun_basics_primer.pdf.

[3] P. Kim, W. Qi, G. Chaudhary, and Y. Jeong, "A Design of Balun Bandpass Filter for Wide Stopband Attenuation Base on Stepped Impedance Resonators," in *2018 Asia-Pacific Microwave Conference (APMC)*, Kyoto, Nov. 2018, pp. 1339–1341, doi: 10.23919/APMC.2018.8617286.

[4] C. Lorenz, "'Schaltungsanordnung zum ¨Ubergang von einer symmetrischen, elektrischen Anordnung zu einer unsymmetrischen, insbesondere bei Hochfrequenzanwendungen,'" 603816.

[5] V. K. Purushothaman, E. Klumperink, B. T. Clavera, and B. Nauta, "A Sub-mW All-Passive RF Front End with Implicit Capacitive Stacking Achieving 13 dB Gain, 5 dB NF and +25 dBm OOB-IIP3," in *2019 IEEE Radio Frequency Integrated Circuits Symposium (RFIC)*, Boston, MA, USA, Jun. 2019, pp. 91–94, doi: 10.1109/RFIC.2019.8701860.

[6] Electronics Hub, "Maximum Power Transfer Theorem," *Maximum Power Transfer Theorem*. https://www.electronicshub.org/maximum-power-transfer-theorem/.

[7] V. K. Purushothaman, E. A. M. Klumperink, B. T. Clavera, and B. Nauta, "A Fully Passive RF Front End With 13-dB Gain Exploiting Implicit Capacitive Stacking in a Bottom-Plate N-Path Filter/Mixer," *IEEE J. Solid-State Circuits*, vol. 55, no. 5, pp. 1139–1150, May 2020, doi: 10.1109/JSSC.2019.2959489.

[8] C. Song, I. Lo, and O. Boric-Lubecke, "2.4 GHz 0.18µm CMOS passive mixer with integrated baluns," in *2009 IEEE MTT-S International Microwave Symposium Digest*, Boston, MA, USA, Jun. 2009, pp. 409–412, doi: 10.1109/MWSYM.2009.5165720.

[9] "Lumped LC-balun - Analog/RF IntgCkts," *Lumped LC-balun - Analog/RF IntgCkts*. https://analog.intgckts.com/impedance-matching/lumped-lc-balun/.

[10] "Global Magnetic Components Manufacturer - Coilcraft." https://www.coilcraft.com/.

[11] "RF-ceramic capacitors - Accu P | AVX," *RF-ceramic capacitors - Accu P | AVX*. http://www.avx.com/products/rfmicrowave/capacitors/accu-p/.

[12] J. Wetherell, "Impedance matching network designer," *Impedance matching network designer*. https://home.sandiego.edu/~ekim/e194rfs01/jwmatcher/matcher2.html.

APPENDIX:
Matlab code for calculations:

```
clear all;
R_L = 200;              %load resistance
R = R_L/2;              %split load resistance
R_s = 50;               %source resistance
Q_L = 50;               %Quality factor of inductor
Q_C = 300;              %Quality factor of capacitor
L = 16e-9;
C = 1.6e-12;
f = 1*10^9;             %desired center frequency
w = 2*pi*f;
w0 = 1/sqrt(L*C);
f0 = w0/(2*pi);
R_ind = w*L/Q_L;        %Series resistance due to Q
R_cap = Q_C/(w*C);      %Parallel resistance due to Q
Z_Lideal = 1i*w*L;
Z_Cideal = -1i/(w*C);
Z_L = Z_Lideal + R_ind;
Z_C = Z_Cideal*R_cap/(Z_Cideal+R_cap);

Z_P =
(Z_L*Z_C*(R+Z_L)*(R+Z_C)+R*Z_L^2*(R+Z_C)+R*Z_C^2*(R+Z_L)+R^2*Z_L*Z_C)/(Z_L*(R+Z_L)*(
R+Z_C)+Z_C*(R+Z_L)*(R+Z_C)+R*Z_L*(R+Z_C)+R*Z_C*(R+Z_L));
Z_n3 = R*Z_C/(R*Z_L+Z_C*Z_L+R*Z_C);     %Transfer from Vx to V-
Z_n4 = R*Z_L/(R*Z_L+Z_C*Z_L+R*Z_C);     %Transfer from Vx to V+
H = R_s/(Z_P+R_s);                      %Transfer from Vin to Vx
Hmag = sqrt(real(H).^2+imag(H).^2);
Hplus = sqrt(abs(real(Z_n4)).^2+imag(Z_n4).^2);
Hmin = sqrt(abs(real(Z_n3)).^2+imag(Z_n3).^2);
immin = imag(Z_n3);
remin = abs(real(Z_n3));
argmin = atan(immin/remin);
implus = imag(Z_n4);
replus = abs(real(Z_n4));
argplus = atan(implus/replus);
phaseplus = rad2deg(argplus);
phasemin = rad2deg(argmin);
phasediff = phaseplus - phasemin;
```

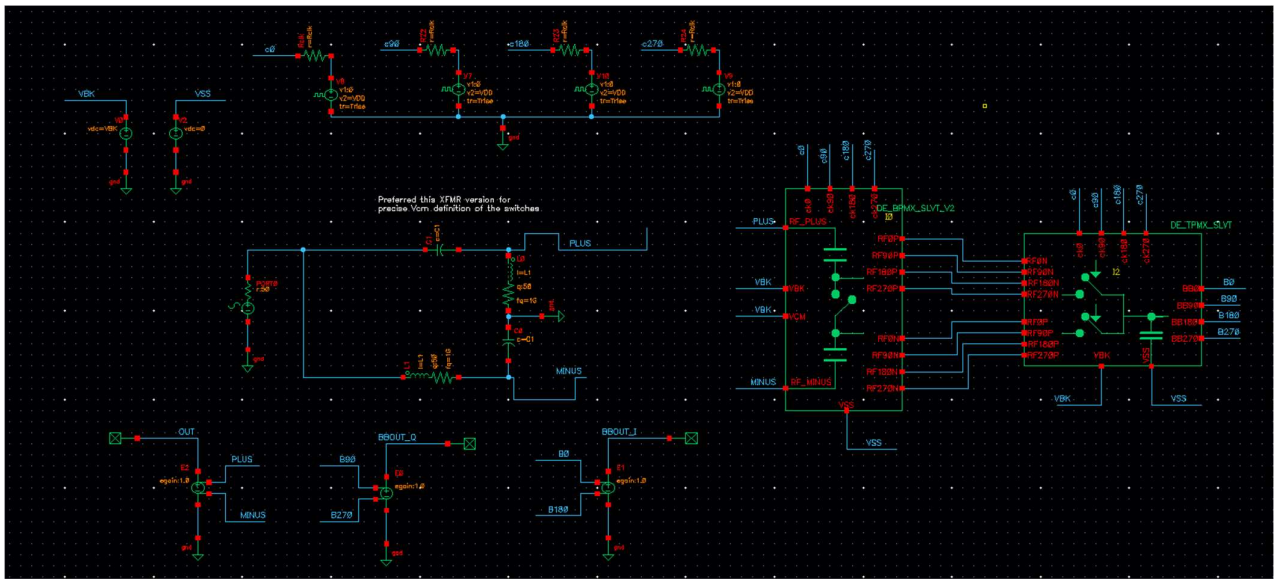
Preferred this XFMR version for
precise Vcm definition of the switches
VBK
VSS
PLUS
MINUS
OUT
BBOUT_Q
BBOUT_I
B0
B90
B180
B270
DE_BPMX_SLVT_V2
DE_TPMX_SLVT
RF_PLUS
RF_MINUS
VCM

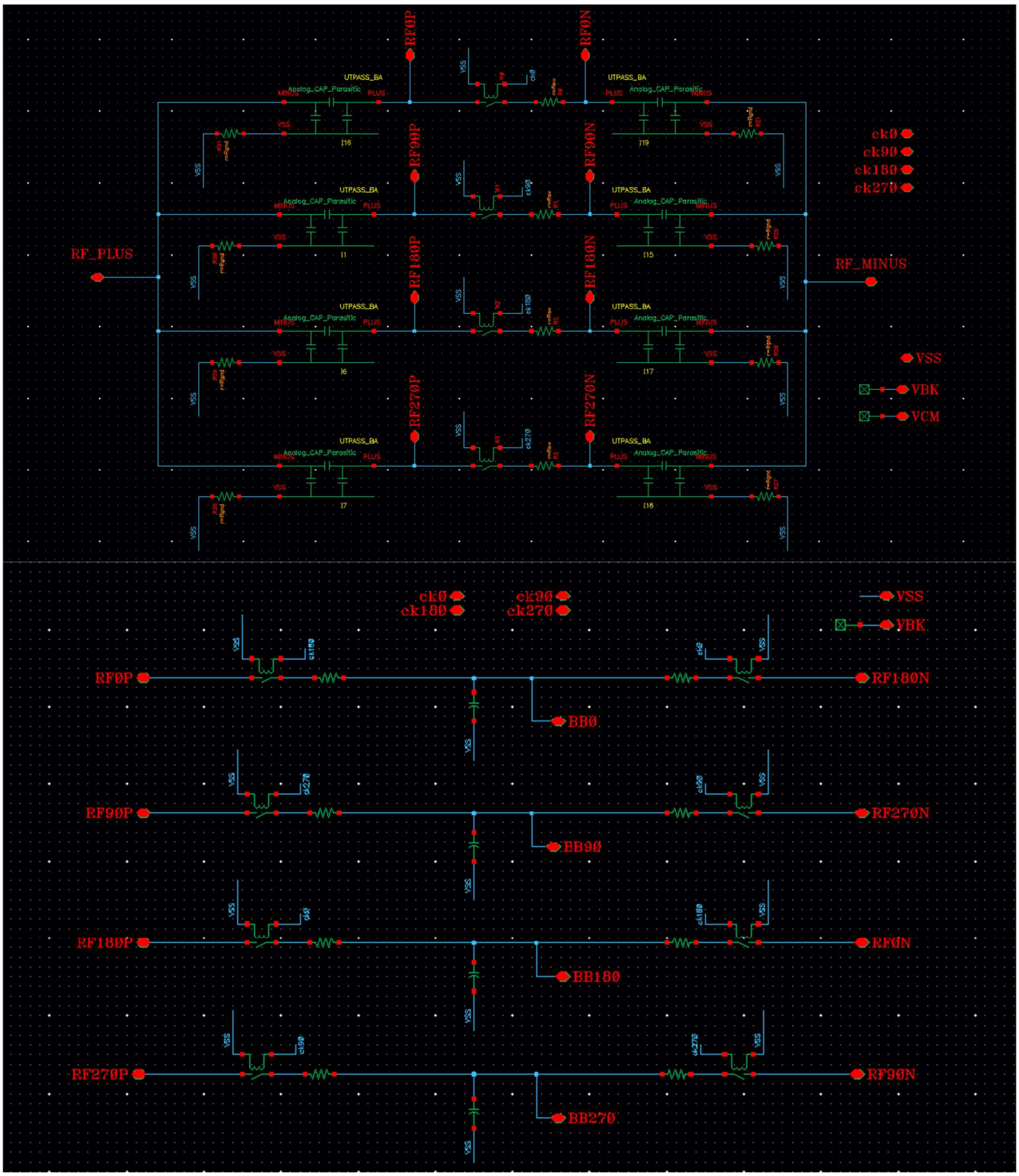
RF0P
RF0N
RF90P
RF90N
RF180P
RF180N
RF270P
RF270N
RF_PLUS
RF_MINUS
ck0
ck90
ck180
ck270
VSS
VBK
VCM
UTPASS_BA
Analog_CAP_Parasitic
PLUS
MINUS
I16
I19
I1
I15
I6
I17
I7
I18
BB0
BB90
BB180
BB270
RF180N
RF270N
RF0N
RF90N